Memoirs of the Faculty of Science, Kyoto University, Series of Physics, Astrophysics, Geophysics and Chemistry, Vol. XXXVIII, No. 2, Article 3, 1992

Movements of the Yamasaki Fault, Southwestern Japan, Inferred from Precise Geodetic Measurements

By

Kunio FUJIMORI

Department of Geophysics, Faculty of Science, Kyoto University

(*Received December 27, 1991*)

Abstract

Movements of the Yasutomi fault, which is one element of the Yamasaki fault system in the Kinki District of Japan, were monitored by employing precise geodetic measurements once a year during the period from 1975 to 1989. The measurements were performed on a baseline network established across the fault in a centered pentagonal shape with diagonal lines of about 300 meters. Combining the results of present measurements with geomorphological studies, geological fault investigations, seismic activity around the fault, results of large-scale geodetic measurements covering the Yamasaki fault system, and results of extensometric observations across the fault fracture zone, the movements and properties of the Yasutomi fault are discussed.

Non-uniform spatial and temporal strain distribution as well as strain accumulation and release exist in and around the fault zone. These phenomena are caused by the low magnitude of the modulus of elasticity of the fault fracture zone as compared with that in its surrounding crust and the plastic flows occurring within the violent fracture zone. The plastic flows may start when the stress in the fracture zone exceeds a critical stress prior to the occurrence of an earthquake. The Yasutomi fault has a wide fracture zone which is thought to be a sheared zone. The minute topography within the fracture zone is a good indicator of the type of fault movement since the movement continues to shape the topography. Such movements are probably linked to small and moderate earthquakes that occur nearby the fracture zone and are interpreted to consist of seismic cycles proposed by Lensen (1971). The narrow width length of the sheared zone and the small scale topography show that the cyclic movements occur only in the shallow part of the fault zone.

1. Introduction

The repetition of geodetic measurements, which are performed by triangulation, trilateration, levelling and/or trigonometric levelling, is one effective way to investigate crustal movements. As a result, it has been clearly shown that the current crustal movements are the continuation of those in the Quaternary period, and that sites with a large amount of movements coincide with those which suffered large earthquakes (e.g., Hayashi, 1969; Nakane, 1973a). At the same time, the locations and dislocations of faults caused by earthquakes are also deduced from crustal movements associated with those earthquakes (e.g., Fitch and Scholz, 1971; Ando, 1971). Further, geomorphological and historical studies on large earthquakes as well as trenching investigations have revealed that large earthquakes occurred

along active faults, and have given the time intervals of slippage and the mean slip rates caused by recurring earthquakes (The Research Group for Active Faults, 1980).

Since large earthquakes occur along active faults, clarifying the state of strains in and around active faults, recognizing strain changes, and discovering the mechanisms of the changes are important for investigating fault movements associated with earthquakes. In this regard, repeated measurements of geodetic networks and continuous observations with extensometers or creep meters have being carried out in and across several active fault zones in the world. In particular, aseismic slippages or creep movements of several centimeters per year have been observed along the San Andreas fault, California, USA, which is a transform fault at a plate boundary (e.g., Savage and Burford, 1973; King et al., 1987). It was also confirmed that some sites along the long fault are locked against creep movements (e.g., Thatcher, 1979). In China, it was reported that some fault movements before large earthquakes were detected from short-distance levelling measurements across faults (Zhang and Fu, 1981).

However, whether creep movements generally exist along active faults or instead take place during a moderate or micro earthquake, has not yet been clarified in inland Japan. The width, physical properties and behavior of fracture zones of active faults have not yet been determined in most cases. In order to investigate fundamental problems of active fault movements, measurements of strains at a medium scale (several hundred meters long) between ordinary large-scale geodetic measurements covering several kilometers, and continuous observations with extensometers (several ten meters long) on fracture zones of faults are necessary. But, such measurement networks with a several hundred meters' scale had been rare because painstaking work and high accuracy are required. The Yasutomi-Usuzuku baseline network established on the Yamasaki fault system is one of special cases (for a case: Kinugasa, 1981). The Yamasaki fault system is a suitable field to investigate the relationship between seismic activity and fault movement, because of the frequent occurrence of microearthquakes as well as some moderate size earthquakes. In 1978, the Yamasaki fault system was designated as a test-field for the National Project of Earthquake Prediction in Japan, and various kinds of measurements and investigations have been carried out there (Kishimoto, 1981, 1987).

The Yamasaki fault system is located in the northwestern part of the Kinki District and is a left-lateral active fault with an upheaval on its northeastern side. It extends approximately 80 km in the NW-SE direction, as shown in Fig. 1. Clear left-lateral offsets of fault movements with inflected ridges and valleys are found at some sites in the fault system. The fault system consists of many fault segments named as the Ohara, Hijima, Kuresakatoge and Yasutomi faults (The Research Group for Active Faults, 1980). The baseline network was established across the Yasutomi fault, and its strike is WNW-ESE which is approximately 20° different from the strike of other faults within the Yamasaki fault system.

In the first half of the present paper, results of the measurements obtained from 1975 to 1989 and their accuracy are given along with the general characteristics of strain and height changes measured in the baseline network. The relationship

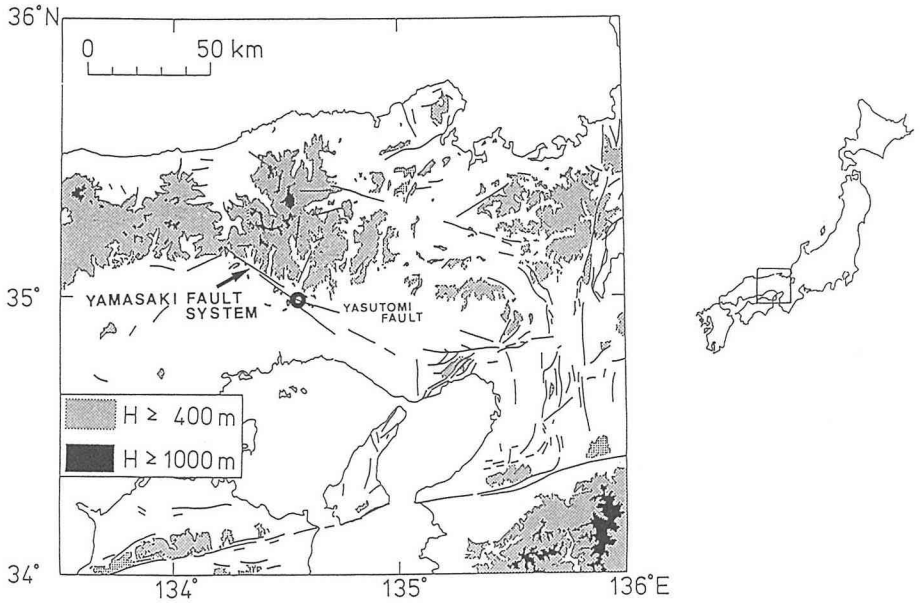

Fig. 1. A map of the northwestern part of the Kinki District, Southwestern Japan. An open circle indicates the Yasutomi-Usuzuku Baseline Network. Solid lines show major active faults.

between the results and seismic activities near the network is also discussed.

In the last half of this paper, the properties of the fracture zone of the Yasutomi fault are discussed from the foregoing results and are compared with geomorphological studies, geological fault investigations and the results of geodetic measurements in the area concerned, as well as the results of continuous observations with extensometers in an underground observation tunnel.

2. Measurements

2.1 Baseline Network

A baseline network, Yasutomi-Usuzuku baseline network, was established at Usuzuku in July 1975 (Fujimori et al., 1981; Omura et al., 1988). At this site, the topographical left-lateral offsets are clearly seen and the network lies across this offset, as shown in Fig. 2. The network formed a centered pentagon with diagonal lines of about 300 m. Each geodetic monument of size 40 cm × 40 cm and 80 cm in height was made of reinforced concrete. Its basement was also made of reinforced concrete. Stations 1 and 2 are located on a ridge inflected by left-lateral movements of the fault and form both ends of the baseline of length approximately 75 m. Intermediate stations A and B for baseline measurements by baseline tapes are located between stations 1 and 2 at an interval of approximately 25 m. Stations 3 and 4 are located on ridges of the southern part and are stations 5 and 6 on flanks at the north of a valley. The Chugoku Expressway runs along the fault. The expressway was constructed by cutting a ridge into the two ridges on which stations

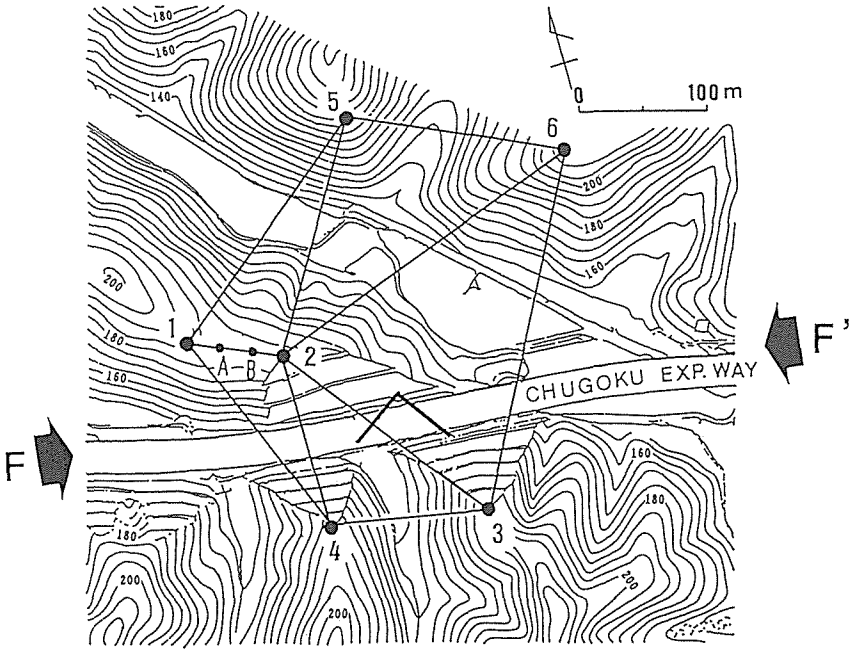

Fig. 2. The arrangement of six stations forming a centered pentagonal network. Large solid circles with numerals indicate stations for triangulation and trilateration. Small solid circles, designated by A and B, are intermediate stations for baseline measurements with baseline tapes. The Yasutomi fault is shown by two thick arrows labeled F and F'. The thick L shape shows the location of an observation tunnel of Yasutomi station.

1 and 2, and station 3 were located, respectively. The Yasutomi observation tunnel, where continuous observations of crustal movements have been carried out by extensometers, is located about 8 m beneath the road surface.

2.2 Methods of Measurements

Measurement methods should be carefully selected in order to achieve an accuracy for distance and relative height measurements among stations with an error limit of 1 mm; this accuracy is necessary for detecting minute fault movements. When the measurements began in 1975, the first order triangulation was the best method for achieving this accuracy. This method includes baseline measurements using several invar baseline tapes and horizontal and vertical angle measurements by employing a Wild T3 theodolite. In addition, "the method of measuring neighboring angles", which was described by Dragomir et al. (1982), was introduced for horizontal angle measurements. The following items were applied to improve the measurement accuracy:

(1) At least two baseline tapes should be calibrated by the Japan Measurement Association just before measurement.

(2) The setting error of measurement instruments and targets should be 0.1 mm or less with the use of special attachments.

(3) The angle measurements should be carried out at night to avoid heat waves caused by the sun and to improve collimation accuracy.

(4) The measurements should be performed at least once a year and should be repeated during the same season in each year in order to avoid the effect of seasonal crustal movements.

The measurements have thus been executed since 1975. The three measurements in the first three years were carried out at the beginning of December and those after that have been carried out at the end of November.

The measurements in 1988 and 1989 were performed by employing a Geomensor CR204 and two invar baseline tapes. These measurements were executed in the daytime. Further, measurement values obtained by the Geomensor CR204 were reduced for errors due to the instrument constant and the elevation angle by comparing them with those measured by using invar baseline tapes at the baseline 1-A-B-2 (Omura et al., 1989).

3. Results

3.1 Accuracy of Measurements

The data obtained in 1975–1989 were analyzed by free network adjustments, based on the coordinates determined in December 1975. Station 1 was fixed in the height estimation. The results obtained are summarized in Table 1. The standard deviation for baseline measurements did not exceed 0.1 mm for baseline 1–2 which was about 75 m long, as shown in Table 1. The triangulations and trigonometric levellings were performed with an error less than 1.1 mm in adjusted values of the coordinates, although a slight fluctuation in precision was seen year after year. In particular, the standard deviations for the trilaterations in 1988 and 1989, which employed the Geomensor CR204, did not exceed 0.2 mm in the

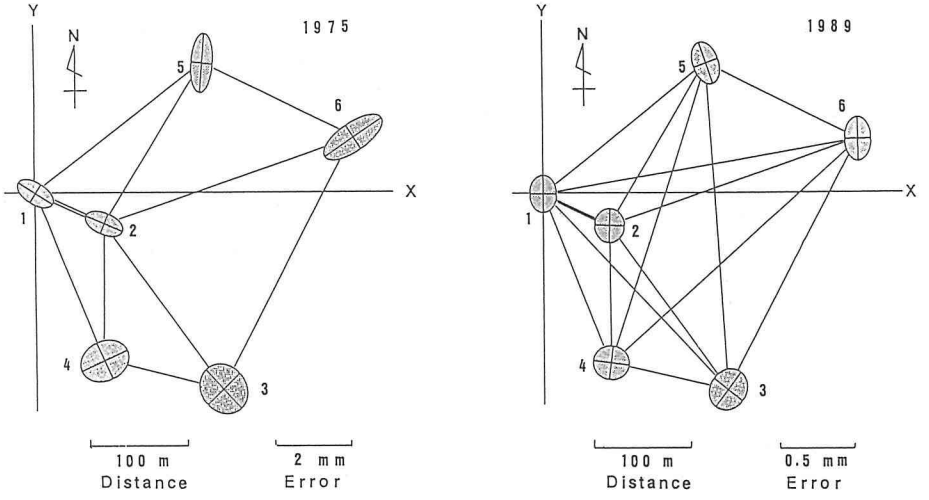

Fig. 3. Error ellipses for 1975 triangulation (left) and 1989 trilateration (right), indicating one standard deviation, determined for each station applying the least squares method.

horizontal coordinates. As a whole, the precision of the trilaterations was about 3 or 4 times higher than that of the triangulations. The error ellipses of the measurements performed in 1975 (triangulation) and 1989 (trilateration) are shown as examples in Fig. 3.

The causes of measurement errors for the triangulations are siscussed in the next section.

3.2 Major Causes of Measurement Errors

In the results shown in Table 1, the misclosure of triangle 152 (△W5) tends to be negative. It was -1.3 ± 0.5 seconds, corresponding to the mean value of thirteen horizontal angle measurements performed from 1975 to 1987, while that of the others did not exceed ± 0.3 second, as shown in Fig. 4. The source of these errors is considered to be that baseline 1–5 runs along the edge of the mountain, and that station 5 is located on a slope facing south. That is, an optical path runs through the atmosphere with some horizontal temperature gradient and therefore the optical path is refracted. Therefore, baseline 1–5 will inflect to make the values of angles 152 and 215 smaller than their true values. The setting around station 5 is not appropriate for such measurements, which is clear from the fact that the precision of the distance measurements from station 5 to other stations by the Geomensor CR204 was inferior even to that for daytime measurements in 1988 (Omura et al., 1989).

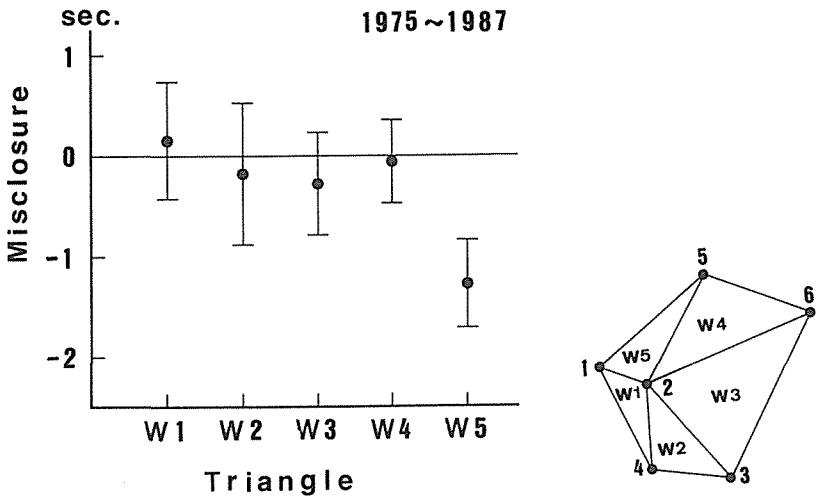

Fig. 4. Mean misclosures of triangulations in 1975–1987 for triangles W1 to W5. An inset shows the layout of the triangles. The bars on either side of the plotted point represent a SD.

The misclosure of triangle 152 may cause a larger and systematic error in the results for the triangulations. However, there were no significant differences between the results of triangulation in 1987 and those of trilateration in 1988 (see Table 1 and Fig. 5). Therefore, it is concluded that there was no systematic error in the

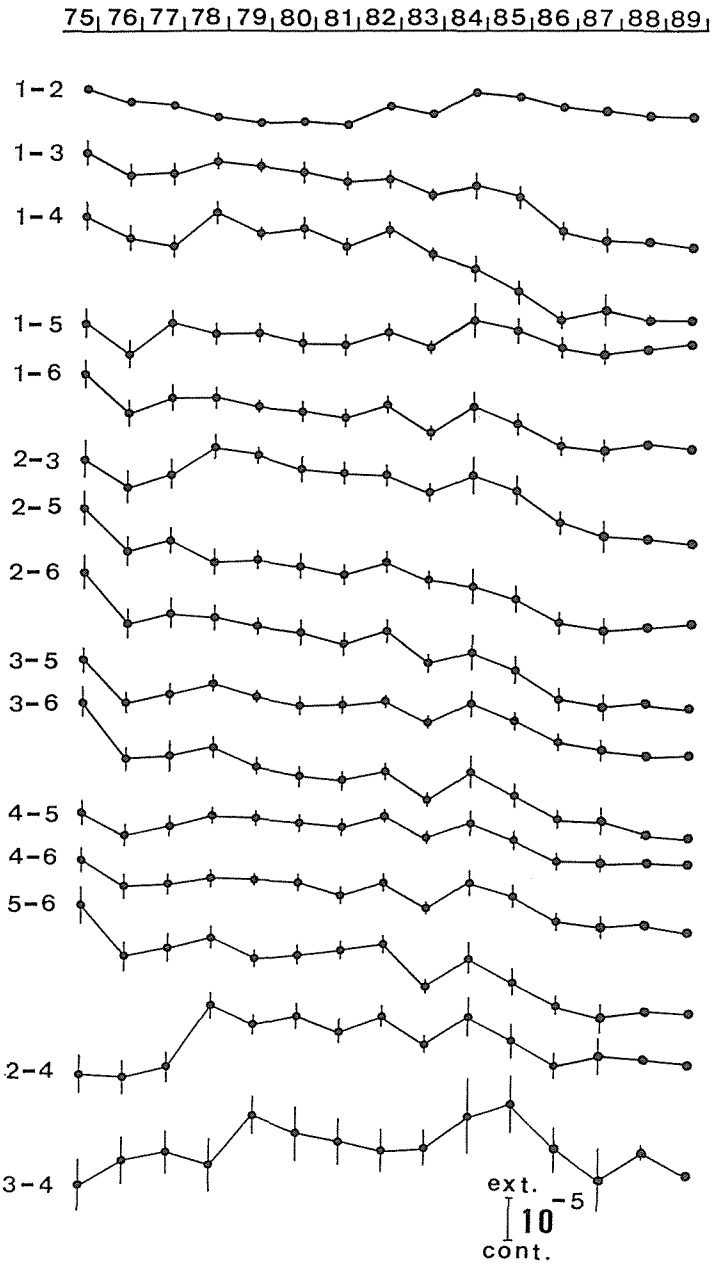

Fig. 5. Secular strain changes of each baseline. The baselines are represented by two terminal stations numbers hyphenated (viz., 1–2, 1–3, etc.).

triangulations. It is probable that the effective precision of the triangulations is higher than the precision shown in Table 1 and Fig. 5.

Refraction coefficients obtained by vertical angle measurements are shown in Fig. 6. Each value for the coefficients was determined as an unknown parameter

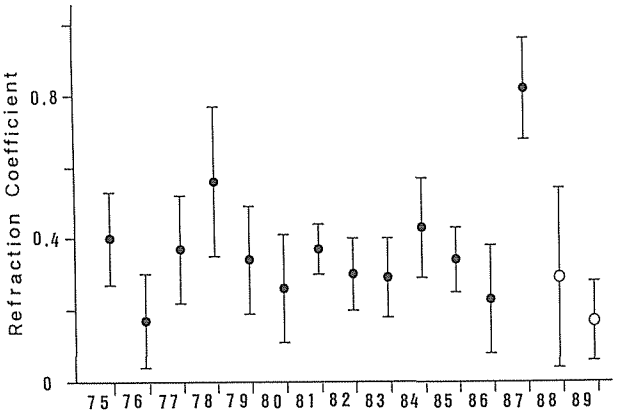

Fig. 6. Refraction coefficients obtained by vertical angle measurements. Closed and open circles denote the values at night and daytime, respectively.

in the network adjustments under the assumption that the value was constant during the course of one set of measurements. The mean value for the thirteen times executed from 1975 to 1987 was about 0.3. The value of the refraction coefficient is ordinarily taken to be 0.15 in the daytime and that in the nighttime is usually larger. The value (0.3) obtained in the nighttime by the present measurements is slightly larger than usual values. In addition, the precision of the vertical angle measurements in 1988 and 1989 was inferior to that before 1988, and therefore the refraction coefficient in the daytime cannot be discussed.

As mentioned above, the effect of optical refraction due to the inhomogeneity of temperature distribution in the atmosphere is so violent that it cannot be neglected in the measurements of horizontal and vertical angles performed in mountain areas.

Another major cause of the measurement errors is due to the shape of the network. In order to increase measurement accuracy, the baseline 1–2 measured with invar baseline tapes is indispensable for the network. The shape of the network is severely restricted by the topography. For this reason, the angles 152 and 241 came to 20.5° and 22.5°, respectively. Such small angles are not ordinarily used for triangulations because measurement errors for such angles produce large errors for the adjusted baseline lengths.

4. Secular Changes of Crustal Movements

In the resulting measurements, the maximum value for length changes was 9.1 mm for baseline 3–6, and for height changes, it was 2.9 mm for baseline 2–6 during 14 years (1975–1989). Although those values were small, they exceeded the measurement errors. Even if the measurements were performed with a high accuracy, the instability of the monuments prevents us from monitoring actual crustal movements. Furthermore, topographic and meteorological influences on the local deformation of the crust affect the estimation of tectonic crustal movements.

Unfortunately, the network has only six stations, and its measurements are being carried out only once a year. Therefore, it is impossible to eliminate all the disturbances from the observed crustal movements. However, in the present study, seasonal disturbances must have been greatly reduced because of measurement in the same season every year.

In this section, the features in the results are described first, and the instability of the stations is then discussed.

4.1 Horizontal Strain Changes

Strain changes of each baseline were obtained, referring to the baseline lengths determined in December 1975. Figure 5 shows the strain changes of all baselines in the network. The strain change of each baseline to the direction angle of the baseline during the period from 1975 to 1989 is shown in Fig. 7. As shown in this figure, the strain distribution in the network is very much non-uniform, and, as shown in Fig. 8, this is seen more clearly in the strain tensors of the triangles with station 2 as one of vertices in the network. The directions of the principal strain axes are nearly NE-SW and NW-SE. The strains in the NE-SW direction show a contraction in the northeastern part of the network and an extension in the southwestern part of the network. The difference in strains in the NE-SW direction between both parts is remarkable. However, the strains in the NW-SE direction are 2 or 3 $\times 10^{-5}$ in both parts, with no great difference.

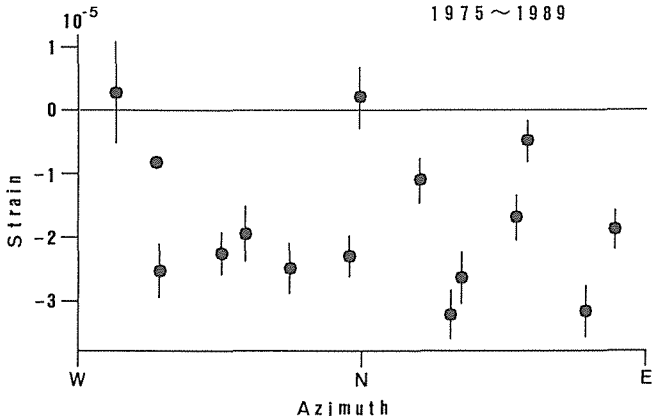

Fig. 7. Relationship between the strain change of each baseline and its azimuth in 1975–1989.

To understand spatial and temporal strain distributions within the network, annual strain rates and accumulated strain tensors based on strain changes were estimated in the various parts of the network as shown in Fig. 9: the northeast (quadrilateral 2563), the southwest (quadrilateral 1234) and the northwest (quadrilateral 1564) parts and the whole network (pentagon 15634). Non-uniform strain accumulations are also remarkable here. Further, the strain tensors of the whole network can be obtained from the strain changes in the five diagonals of

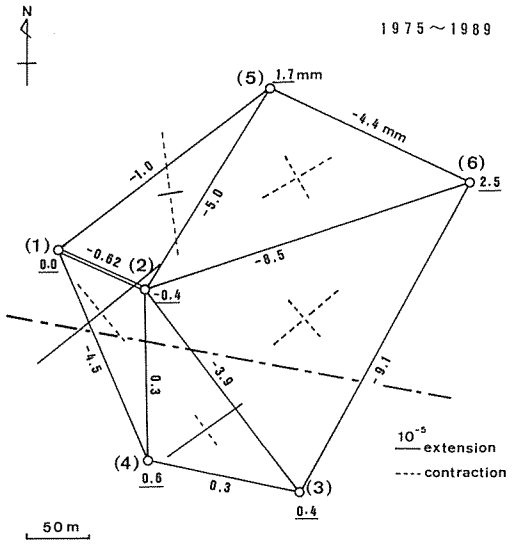

Fig. 8. Strain tensors in the network during the period from 1975 to 1989. Numerals attached on each line show length changes. Numerals on the station marks indicate the height changes of the stations relative to station 1. A dash-dotted line denotes the trace of the Yasutomi fault.

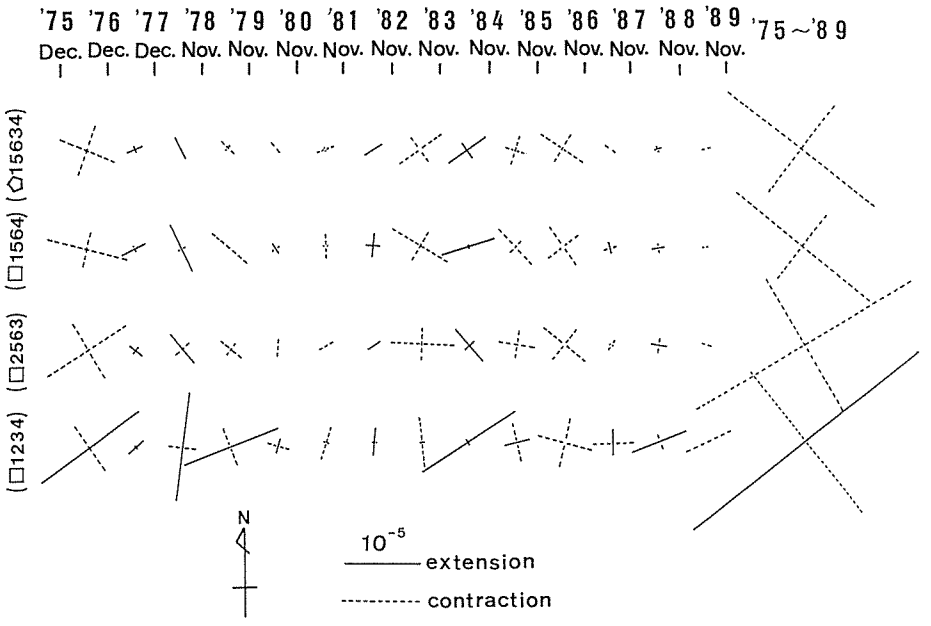

Fig. 9. Annual strain rates (left) and accumulated strains (right) for the pentagon (top) and each quadrilateral (bottom) in the network. The strains for the pentagon were estimated based on the strain changes of the five diagonals.

pentagon 15634. The reason why only the diagonals were employed is that the longer the baselines are, the smaller the effect caused by the instability of the monuments and the local distribution of strains. As to the strain pattern of the whole network during the period of about 14 years, the directions of the principal strain axes were also NW-SE and NE-SW with contractive changes of about 2.5×10^{-5} and 1.5×10^{-5}, respectively.

The characteristics of the strains observed in the network during the period from 1975 to 1989 are summarized as follows:

The strain changes were contractive in the NE-SW direction in the northeastern part, whereas they were extensional in the NE-SW direction in the southwestern part. The strain changes in the whole network were contractive in the NW-SE direction of the major principal strain. Further, the strain changes during the 14 years showed that the tendency of the strains in 1975–1976 has continued, accumulated and enlarged from that time on, as shown in Fig. 9. The estimated mean strain rate in the network was on the order of 10^{-6} per year.

4.2 Horizontal Displacement Vectors

When considering the change of horizontal displacement vectors, careful attention should be paid so that the pattern of the vectors varies according to the fixed station and fixed direction, because a rotation is included. To avoid the

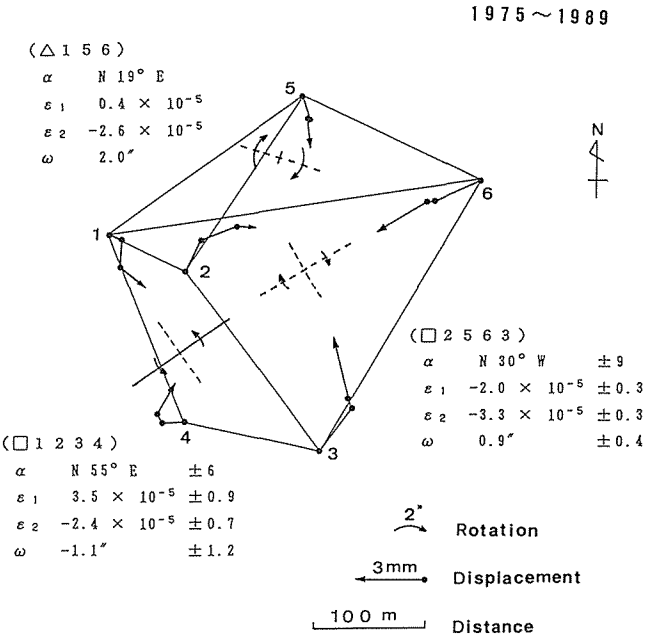

Fig. 10. Horizontal displacement vectors of the stations. The values in 1980, 1985 and 1989 are shown in this figure, for which that in 1975 was adopted as the base. Strain tensors and rotations during the period of 1975–1989 determined from the horizontal displacements are also shown with their values.

effects of fixed station and fixed direction, free network adjustments are applied in data processing.

The results are shown in Fig. 10. Values in 1980, 1985 and 1989 are shown in the vectors, and that of 1975 was adopted as the base. In this figure, the displacements toward the NE direction at stations 2 and 3, and those toward the SE direction at station 6 are remarkable. This figure also shows the strain tensors and rotations obtained from the vectors at stations 1, 5 and 6, stations 2, 5, 6 and 3, and stations 1, 2, 3 and 4.

As shown in this figure, the strain distribution in the network trends as follows:

(1) There was a uniaxial compression nearly parallel to the strike of the Yasutomi fault in the northern part.

(2) There was shear strain with a severe left-lateral offset movement between stations 1 and 2 as well as between stations 3 and 4.

(3) There was a remarkable extension and contraction in the NE-SW direction in the southwestern and northeastern parts, respectively.

(4) The southern part (stations 3 and 4) rotated in a counterclockwise by 2 to 3 seconds relative to the northern part (stations 1, 5 and 6), and the distance between both parts became smaller.

4.3 Height Changes

Figure 11 shows the height change of each station for which station 6 was

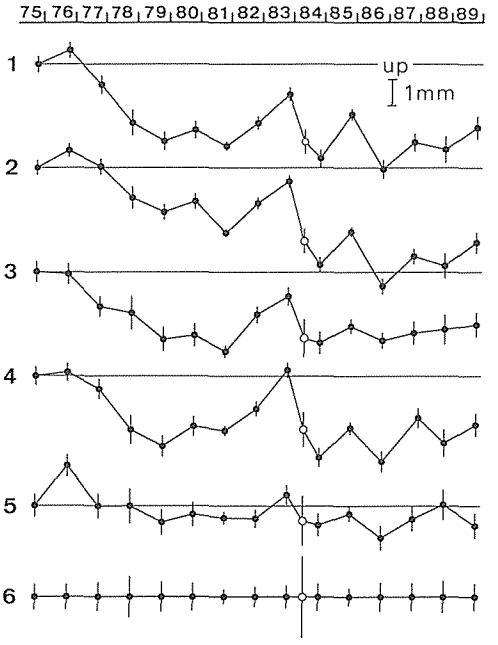

Fig. 11. Height changes of respective stations referred to station 6 which was assumed to be unchanged. Open circles denote the values obtained by the measurements in June 1984, one week after the earthquake (M = 5.6) on May 30, 1984.

fixed. Open circles indicate the values measured one week after the earthquake (M = 5.6) that occurred on May 30, 1984.

Although the pattern of changes for each station is different, stations 5 and 6 located in the northeastern part of the network show an overall upheaval of about 2 mm relative to stations 1, 2, 3 and 4 in the southwestern part. Under the assumption that the network tilts uniformly, the maximum tilt direction and its magnitude were obtained to be WSW and about 6×10^{-6} radians, respectively, during the 14 years (see Fig. 14). The undulation of the tilt is considered to have relation with the earthquake, which will be mentioned later.

4.4 Changes of Baseline 1-A-B-2

The length of baseline 1-A-B-2 was measured by employing several baseline tapes as the base for triangulations or trilaterations. These four stations on the baseline are at equal intervals, but the deformation patterns were different at each section.

Figure 12 shows the changes of lengths among stations 1, A, B and 2. Baselines 1-A and B-2 showed an inverse correlation, such that when the length change of the one baseline was extensional, that of the other one was contractive. Baseline A-B showed a contraction in 1977–1978 with no other significant changes in any other period. Stations A and B shown in Fig. 13 also upheaved relative to stations 1 and 2: Baselines which changed in length changed also in relative height. Although the change between stations 1 and 2 were not uniform, the distance between both

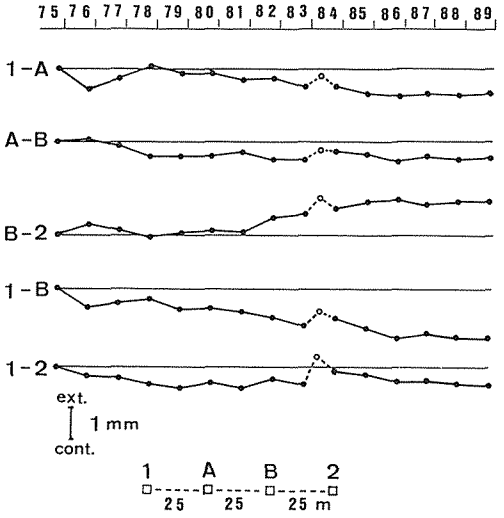

Fig. 12. Secular changes of baseline length 1–2 and its segments. Arrangement of stations on baseline 1–2 is shown as an inset. Open circles are the same as in Fig. 11. The standard deviations of all points plotted are smaller than the size of circles themselves.

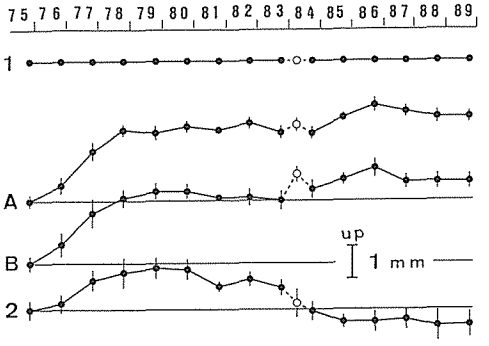

Fig. 13. Height changes of stations A, B and 2 referred to station 1. Open circles are the same as in Fig. 11.

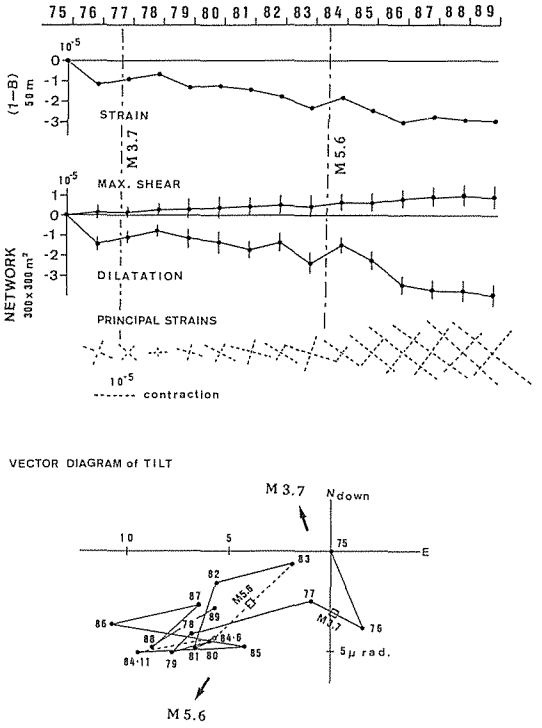

Fig. 14. Comparison of crustal movements observed and seismic activity near the network. From top to bottom, secular strain changes of segment 1-B, maximum shear strain and dilatation changes and accumulated strains of the pentagon 15634, and a vector diagram of tilts are shown in this figure. Vertical dash-dotted lines in the upper part and open squares in the vector diagram indicate the time of moderate earthquakes which occurred at epicentral distances of about 3 km. Thick arrows point toward their epicenters.

stations was shortened, and their intermediate parts rose relative to the both ends.

These changes are similar to those of the network in the following way. An excellent correlation is found between the strain change of baseline 1-B and dilatation change obtained using five diagonals of the network, as can be seen in Fig. 14. Comparing Fig. 5 with Fig. 12, it can be also noted that the length change of baseline 1-B correlates with the strain changes of most of the other baselines. In addition, the senses of strain changes of baselines 1-A and B-2 are reversed just as in that of the strains in the NE-SW direction in the northeastern and southwestern parts of the network.

These facts show that the strain changes obtained by the repetition of triangulations or trilaterations are sufficiently reliable.

4.5 Non-Uniformity of Strain Distribution

According to the results, the strains of the NE-SW direction in the northeastern part (stations 3, 2, 5 and 6) of the network and those in the southwestern part

(stations 1, 2, 3 and 4) show a reversed sense. It is necessary to examine the cause of such a phenomenon and whether it was due to the instability of the monuments themselves or not.

Figure 8 shows that the patterns of strain tensors are similar within the northeastern part and also the southwestern part. As shown in Fig. 10, the strains estimated from the horizontal displacement vectors have small standard deviations. This means that some of the three groups of the stations (i.e., 1 and 4, 2 and 3, and 5 and 6) must have moved toward an identical direction. If the strain near the fault corresponds to that of the wide area, then the displacements of stations 1 and 4 do not correlate. However, the strain change of baseline 1-B is similar to the dilatation change of the whole network and the strain changes of most of baselines as shown Figs. 14 and 5, respectively. The directions of the principal strain axes in the northeastern and southwestern parts of the network correspond to each other as shown in Fig. 10. From these facts, it is difficult to conclude that displacements of the stations 1 and 4 are anomalous.

On the other hand, results obtained from the continuous observations of crustal movements in fracture zones of faults revealed a similar phenomenon. It was reported that senses in strain accumulation differed in the same direction, as taken from array observations employing extensometers installed in the tunnels crossing the Yasutomi fault (Watanabe, 1991) and the Otsuki fault (Otsuka et al., 1982). Particularly for the Otsuki fault, the strains measured with an extensometer installed across the fracture zone where fault clay is clearly observed showed an opposite sense to those measured with other extensometers even in the case of earth tidal strains (Tanaka et al., 1972). A secular strain rate observed in the Otsuki fault was on the order of 10^{-5} per year, which is larger than that from the measurements discussed in the present paper.

The fracture zone of a fault, especially its ground surface, is an area in which destroyed rocks are supposed to exist and for which the theory of elasticity for a uniform strain is not supposed to be applied. It is considered that results obtained by measurements vary depending on the characteristics of each fault, such as rate of slip, width of fracture zone, the location of each station within or outside the fracture zone and others.

From these considerations mentioned above, the difference in strain distribution measured in the network is the result of variation within the fracture zone itself rather than the result of a coincidental instability of the monuments.

5. Relationship with Seismic Activity

5.1 Seismic Activity around the Network

Seismic activity around the Yamasaki fault system is very high and microearthquakes, including some moderate earthquakes, occur along the fault system. The recurrence interval of moderate earthquakes is approximately every eleven years (Tsukuda, 1985). According to Kishimoto and Nishida (1973), the focal mechanism of earthquakes that occur along the Yamasaki fault system has a

characteristic feature; that is, the direction of a nodal line is the same as the strike of the segment faults. Thereofore, earthquakes occurring on the Yasutomi fault can be distinguished from those on other faults in the Yamasaki fault system because of the difference in fault strikes. In addition, there is a historical document on an earthquake ($M \fallingdotseq 7$) which occurred in 868, and the fault movement caused by this earthquake was confirmed in a trenching investigation (Okada et al., 1980).

Earthquakes ($M > 3.5$) which occurred on and around the Yamasaki fault system during the period concerned (1975–1989) are shown in Fig. 15. In the vicinity of the network, two earthquakes occurred on September 30, 1977 ($M = 3.7$, $\Delta = 3$ km, $H = 20$ km) and on May 30, 1984 ($M = 5.6$, $\Delta = 3$ km, $H = 19$ km). Three earthquakes whose epicenters were located in the west and east about 20 km from the network occurred during the period from October 1979 to January 1980.

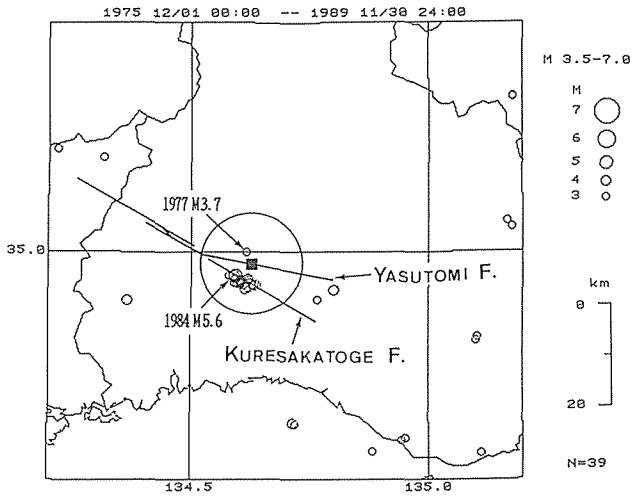

Fig. 15. An epicentral map around the Yamasaki fault system during the period of the present study. Small open circles denote epicenters ($M > 3.5$). A Closed square indicates the network. A large open circle represents an area with a radius of 10 km from the network. The data of the earthquakes were obtained using the program "SEIS-PC" (Ishikawa et al., 1985 and supplemental data).

Earthquakes larger than $M = 3.5$ having epicentral distances less than 10 km from the network during the period from 1950 to 1989 are shown in Fig. 16. Seismic activity near the network had been high during the measurement period because of no such earthquake in any other period except 1961.

Further, the earthquake which occurred in 1977 had the focal mechanism shown at the bottom (left side) of Fig. 17. This earthquake is considered to have relation with the Yasutomi fault and to have occurred beneath the network. The 1984 earthquake had the focal mechanism shown at the bottom (right side) of Fig. 17 and occurred at the Kuresakatoge fault located to the south of the Yasutomi fault. As shown in Fig. 17, aftershocks ($M > 3.5$) lasted until 1985.

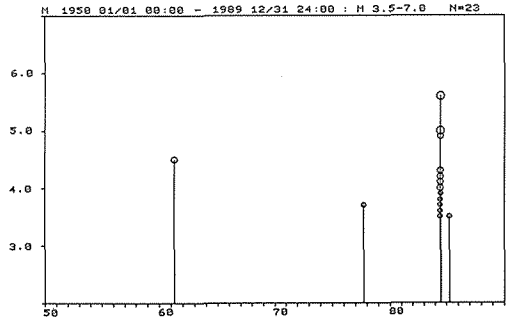

Fig. 16. Seismic activity ($M > 3.5$) in the area within a distance of 10 km from the network during the period from 1950 to 1989. Open circles denote earthquakes. The program "SEIS-PC" was used to draw this figure.

5.2 Fault Movements Associated with Moderate Earthquakes

In Fig. 14, the occurrences of the two earthquakes in the vicinity of the network are shown by dash-dotted lines in the upper part, and they are also marked with open squares in the lower part. The directions toward the epicenters are also indicated by arrows in the vector diagram.

Features recognized commonly in both the dilatation and tilt changes associated with the two earthquakes are as follows:

(1) The dilatation rate about one year before the earthquake occurrence was compressive, while it was expansive in the measurement period including the earthquake occurrence.

(2) An upheaval occurred toward the epicentral direction about one year before the earthquake occurrence and it was recovered in the measurement period including the earthquake occurrence.

On the other hand, because the maximum shear strain showed an almost linear trend, it seems that no significant lateral offset movement of the fault took place at the time of the earthquake.

Now, we will give a detailed discussion of the strain and height changes associated with the two earthquakes. In Fig. 17, the strain rates of pentagon 15634 (the whole network), quadrilateral 2563 (the northeastern part of the network) and quadrilateral 1234 (the southwestern part) are introduced for the strains, and the height changes of baseline 6–3 (the height change of station 6 located in the northeastern part referred to station 3 in the southeastern part) and baseline 6–5 (both stations 5 and 6 are located in the northeastern part) are adopted. The reasons for this is because the distribution of both strain and height changes differs in the northeastern and southwestern parts of the network, and the angle of intersection between baselines 6–3 and 6–5 is almost a right angle.

From the point of view of strain rates and height changes, the period concerned can be divided into two cycles: December 1975–November 1982 and November 1982–November 1989. The strain rates and height changes are relatively large in the beginning of the cycles and small at the end. In each cycle, an earthquake occurred near the network in the second year.

Considering the occurrence of the earthquake, it is considered that crustal movements within one cycle consist of four stages A, B, C and D, as shown in

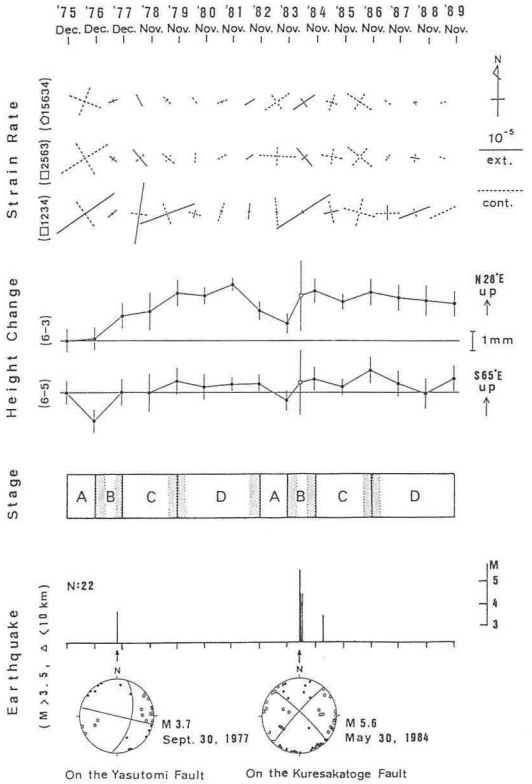

Fig. 17. Comparison of the modes of crustal movements and seismic activity. From top to bottom, annual strain rates (the same as in Fig. 9), height changes of baselines 6–3 and 6–5, seismic stages introduced from the modes of strain rates, height changes and earthquake occurrences, and seismic activities with two focal mechanisms are shown in this figure. The focal mechanisms in 1977 and 1984 were determined by Tsukuda (1978) and Nishida (1985), respectively.

Fig. 17; this concept is related to the idea of a seismic cycle on crustal movements introduced by Lensen (1971). The boundaries of the consecutive stages are not clear because the measurements were performed once a year. For that reason, an allowance range for the boundaries are shown by shadowing.

The relationship between the movements with seismic activity for each stage is as follows:

(1) Pre-seismic stage A shows large strain and height changes.
(2) Co-seismic stage B shows strain release and height change recovery.
(3) Post-seismic stage C shows large strain and/or height changes.
(4) Inter-seismic stage D shows quiet strain and height changes.

It is considered that the difference in deformations after the two earthquakes is due to a difference in locations of the hypocenters to the Yasutomi fault. That is, even though the epicentral distances of the earthquakes were similar, the 1977 earthquake occurred at the Yasutomi fault with vertical offset movements in the

Quaternary period. After the earthquake, the northeastern side of the fault upheaved for a few years relative to the southwestern side. The focus of the 1984 earthquake was located in the Kuresakatoge fault which was different from the fault associated with the network. The aftershocks of the 1984 earthquake lasted for a period nearly equal to the post-seismic stage C.

6. Summary of Measurement Results

Precise measurements of the centered pentagonal network established across the Yasutomi fault have been carried out since 1975. The main features of the measurement results during the period from 1975 to 1989 are summarized as follow:

(1) An inverse correlation was detected between the length changes of baselines 1-A and B-2.

(2) A positive correlation was detected between the strain changes of baseline 1-B and the dilatation change of the whole network.

(3) The strain of the network as a whole was contractive and the directions of the principal strain axes were NW-SE and NE-SW with large changes of about 2.5×10^{-5} and 1.5×10^{-5}, respectively.

(4) The strain distribution in the network differed largely in the northeastern and southwestern parts of the network. In both parts, the strain in the NW-SE direction was contractive. However, the strain in the NE-SW direction was contractive in the northeastern part and extensive in the southwestern part.

(5) In height changes, the relative elevation in the northeastern part was approximately 2 mm with respect to the southwestern part. When a uniform tilt was assumed, the direction of the tilt was WSW and its magnitude was about 6×10^{-6} radians.

(6) A left-lateral movement was detected between stations 1 and 2 as well as between stations 3 and 4.

(7) A counterclockwise rotation of about 2 to 3 seconds was detected in the southern part of the network relative to the northern part.

(8) The strain and height changes were considered to be related to two earthquakes that occurred near the network as follows:

a: The strain showed a contraction and an upheaval toward the direction of the epicenter about one year prior to an earthquake, and it showed an extension and the recovery of the tilt at the time of the earthquake.

b: The two earthquakes that occurred at the Yasutomi fault (1977) and the Kuresakatoge fault (1984) had different after-effects on the strains and tilts of the network.

c: From such modes of strain and tilt changes, the period for the measurements in 1975–1989 was divided into two seismic cycles corresponding to the two earthquakes. One cycle consists of four stages; that is, pre-seismic, co-seismic, post-seismic and inter-seismic.

7. Consideration of Fault Movements

The analysis of the measurement data shows that strain and tilt distributions within the network change spatially and temporally and that the changes in strains and tilts are related to earthquakes in the vicinity of the network. It is considered that those were caused by the wide fracture zone of the fault. The measurement results can thus be explained based on the following assumptions regarding the fracture zone.

(1) In the fault fracture zone, yield stress is so small that a plastic deformation occurs easily.

(2) The violent fracture zone which affects the strains and tilts in the network is located between stations 1, 2, 3 and stations 5, 6; its location corresponds to the valley which trends in the NW-SE direction.

(3) The plastic deformation begins at the time of large contractive strains before an earthquake (abotu one year) and continues for a few years.

Observations of destroyed rocks and fault clay which exist within the fracture zone and the fact that stresses in the crust increase with depth indicate the shape of the fracture zone as shown in Fig. 18; the width of the fracture zone decreases with depth. The fracture zone is found to have a greater plasticity than the surrounding area. Although it is rather qualitative, the fracture zone can be modelled as a plastic body (Bingham substance) which is sandwiched between two elastic bodies, as shown in Fig. 19.

Both elastic and plastic bodies contract under usual compressive stresses. When the stresses within the fracture zone exceed a certain value (σ_0), plastic flow starts. As the plastic body continues to contract, the elastic bodies extend, because of the stress release caused by the flow in the plastic body. As a result, the amount

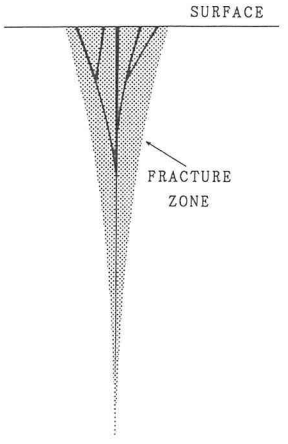

Fig. 18 A possible schematic diagram for the fracture zone of a fault in the vertical section. Thick lines represent violent fracture zones.

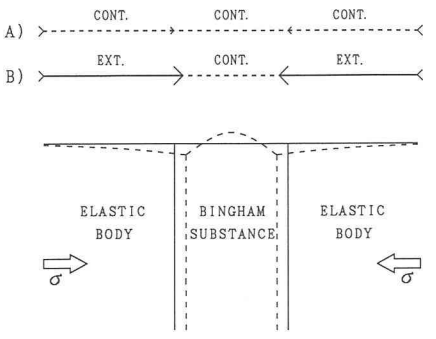

Fig. 19. A simple model of a violent fracture zone. A) and B) show the line distribution of strains before and after the occurrence of plastic flow in a Bingham substance, respectively. Dotted lines in the bottom figure denote deformation caused by the plastic flow.

of strain in the same direction differs greatly, or the sense of the strains begins to reverse. Height changes are also produced as the plastic body becomes higher relative to the elastic bodies. Further, the rate of the plastic flow (i.e., the strain rate) is controlled by its physical properties, but not by stresses (Jaeger, 1964).

In hypothesis (1), the stress value in the fracture zone of the fault is always close to the value of yield stress. The strains in the fracture zone change with stress changes in the adjacent areas, and the strains become larger because of plastic flow in the fracture zone. Such behavior in the fracture zone makes it possible to detect strain changes associated with moderate earthquake. Further, it is considered that strain changes depending upon the physical properties of the fracture zone. If there is a violent fracture zone as in hypothesis (2), it is possible to explain the difference in strains between the northeastern and southwestern parts in the network. It is also considered that the violent fracture zone is located in the southeast of baseline 1–5 (see Fig. 21), because the strain changes of baseline 1–5 were relatively small (see Fig. 5).

Let us now look at this idea from the viewpoint of strain fields in a wide area. Faults exist in many places in the upper crust. The strain distribution will vary to some extent relative to areas where stresses will be released by the plastic flow of faultings, but the depth of the fault is limited. This concept leads to the conclusion that the strains measured by large-scale measurements with long baselines should reflect tectonic stresses more accurately than those by short-range ones. Thus, it is considered that the strains in a relatively small area obtained by continuous observations of crustal movements do not necessarily correspond to those by geodetic measurements. Acceleration of the strains, such as the migration of crustal deformation (e.g., Kasahara, 1979; Ishii et al., 1979) and the phase change of crustal movemens (e.g., Tanaka, 1989) probably has significance as a reflection of tectonic stresses.

In the following section, the measurement results are compared with other data under the assumption of the existence of such a fracture zone as discussed above.

8. Comparison and Examination

8.1 Fracture Zone

Huzita (1969) explained that the origin of the Yamasaki fault system is the E-W compression attributable to the Pacific plate. As mentioned previously, the Yamasaki fault system is a left-lateral active fault with an upheaval on its northeastern side. Based on the stream offsets across the fault, it is estimated that the maximum horizontal dislocation is about 500 m and that the average slip rate is about 0.3 mm/year (Fukui, 1981).

Figure 20 shows the structure of the Yasutomi fault near the network investigated by Hase (Huzita, 1980). In this figure, there are several parallel faults at an interval of about 300 m in the area to the west of the network, while only two faults are described on the east side of the network. It is thought from this figure that the structure of the Yasutomi fault near the network is as follows:

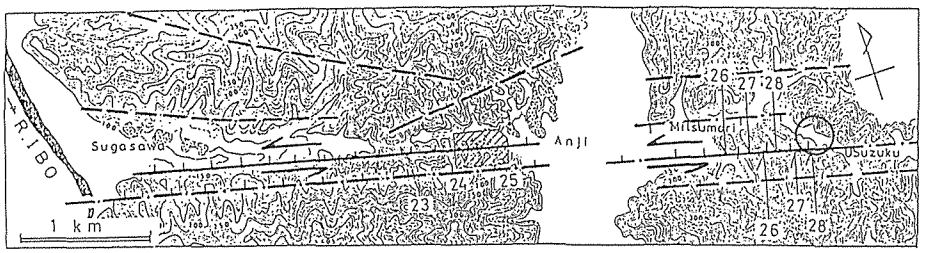

Fig. 20. An echelon arrangement of faults near the network as studied by Hase (after Huzita, 1980). The open circle denotes the network.

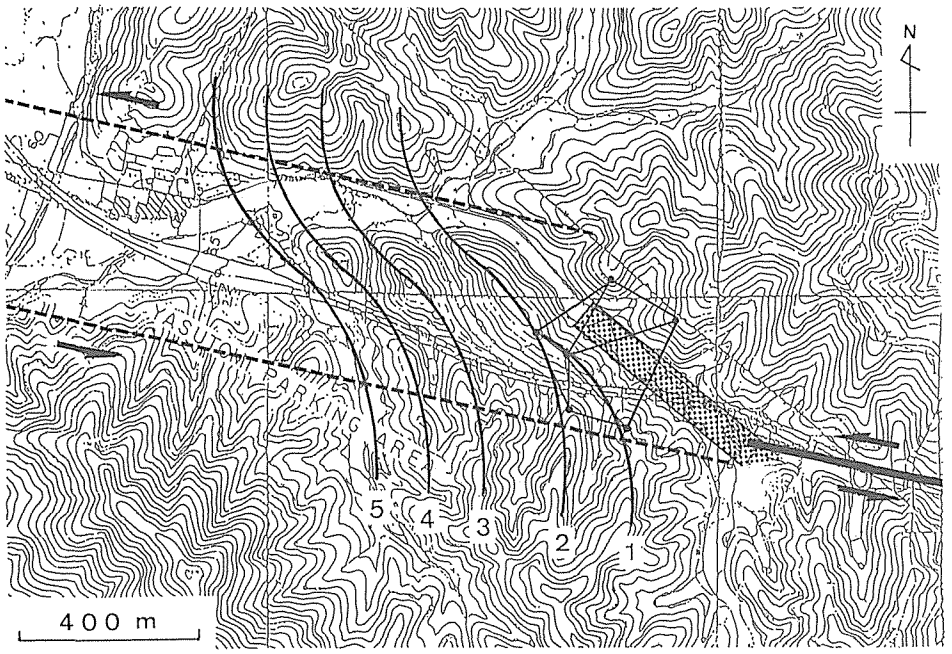

Fig. 21. A topographical map around the network showing the fault movements presumed in the present study. Thin solid lines marked with 1 to 5 denote the supposed connection of the valleys and ridges inflected by the left-lateral fault movement in the sheared zone of the fault. Thick solid and dotted lines show the inferred width of the sheared zones. The hatched zone indicates the location of the inferred violent fracture zone.

The appearance of the fault has changed near the network or faults have kept an echelon with each other in the neighborhood of the network. In the area to the west of the network, movements took place in a wide fracture zone resulting in the inflection of ridges and valleys creating a sheared zone. In the area to the east of the network, movements occurred in a narrow zone. The valley which is lying to the NW-SE direction between stations 1, 2, 3 and stations 5, 6 is the boundary of both areas in the fracture zone. This means that the valley can be regarded as one end of a left-lateral fault, or as a fault that connects two echelon faults. This conception is shown in Fig. 21.

Also, from this topographical map, elevation changes greatly between the both sides of the fracture zone at this valley, and the northeastern side of the valley is higher than the southwestern side. This fact is in agreement with the fact that the northeastern side of the Yasutomi fault has upheaved in the Quaternary period and stations 5 and 6 have upheaved relative to stations 1, 2, 3 and 4 in 1975–1989, as shown in Fig. 11.

Thus, as supported by the topographic consideration, hypothesis (2) mentioned above (that a violent fracture zone which affects the strains and tilts in the network is located between stations 1, 2, 3 and stations 5, 6) is appropriate. The strains obtained for the movements of stations 2, 5, 6 and 3 are considered to most closely reflect the movement of the Yasutomi fault. Moreover, since the fault (a fracture zone) between stations 1–2 and 3–4 is being relatively locked, this fault is expected to move if many echelon faults are dislocated as one fault in the event of a large earthquake.

The assumption that the ridges and valleys are connected in a sheared zone on the western side of the network is depicted by the solid lines marked 1 to 5 in Fig. 21. The fact that the lines 1 and 2 are connected near station 1 is consistent with the measurement results that there are a great difference in displacements between stations 1, 4 and stations 2, 3.

Since the southern part of the network is rotating in a counterclockwise direction relative to the northern part, it is possible for the block indide the fracture zone of the left-lateral fault to also rotate in the same direction. Supposing the rotation rate in the sheared zone is constant at about 0.2 second/year (as determined by the measurements), this amounts to about 50° over the one million years of the Quaternary period, which agrees roughly with the about 45° at which the directions of the ridges and valleys in the sheared zone cross the strike of the Yasutomi fault.

A larger scale inflection of the valleys in the N–S direction crossing the Yasutomi fault is shown by the solid lines 1 to 5 in Fig. 22. On the northern side of the fault, the lines are almost straight until they are inflected to the left on the fault, showing convex curves to east on the southern side of the fault. Intervals between the lines on the northern side of the fault are smaller than those on the southern side. These are thought to be caused by the greater contraction of the block on the northern side of the fault, and it is also thought that this causes the southern side of the fault to rotate against the northern side and to be lower than the northern side. This means that a similar rotation observed in the measurements occurs also in far wider areas along the fault.

The fault movements deduced from such topographical evidence correspond to the upheaval of the northern side of the fault in the Quaternary period and also agree with the crustal movements expected by the secondary geodetic station surveys mentioned later.

Based on the results of electromagnetic surveys, the fracture zone of the Yasutomi fault is as width as approximately 2 km (Electromagnetic Research Group for the Active Fault, 1982) or about 6 km (Handa and Sumitomo, 1985). According to a geological study, there are many normal and reverse faults within the fracture

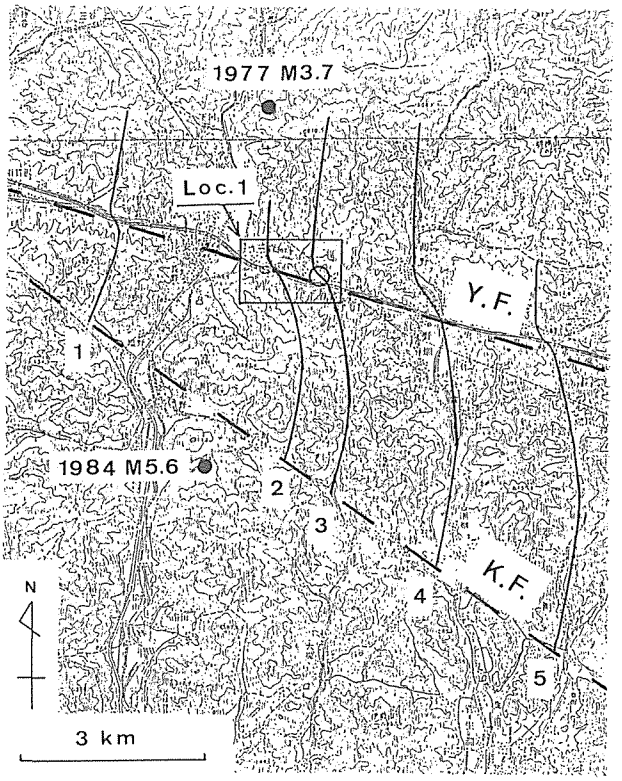

Fig. 22. The inflection of valleys crossing the Yasutomi fault (Y.F.). Solid lines 1 to 5 denote the supposed connection of the valleys on both sides of the fault. Loc. 1 is the same area as in Fig. 21. The Kuresakatoge fault (K.F.) and the two epicenters are also shown by closed circles in this figure.

zone of the Yasutomi fault (Nishimura et al., 1985). These evidences along with the topographical information support the assumption that the fracture zone is relatively with and that there are many small faults in the fracture zone.

The assumptions that the network (size, about 300 m) is located within the fracture zone and that the entire fracture zone, as estimated from the topography, is the source of movements in the network, explain the measurement results excellently.

8.2 Large-scale Measurement Results

The northwestern part of the Kinki District, where the Yamasaki fault system is located, is an area with small strain changes (Nakane, 1973b) and vertical movements (Hayashi, 1969), within Japan. The results of the primary geodetic station surveys during the past 100 years are shown in Fig. 23 (Geographical Survey Institute, 1987). In this figure, there has been no notable strain accumulation along the Yamasaki fault system. The directions of the major contractive strain axes were

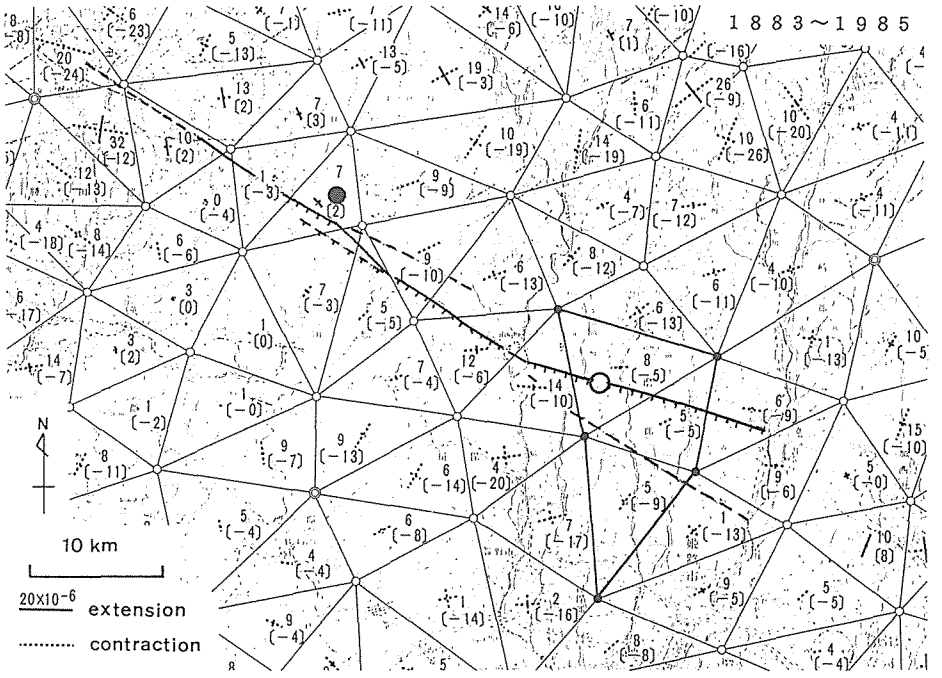

Fig. 23. Horizontal strain distribution obtained using the primary geodetic stations around the Yamasaki fault system during the past 100 years (after Geographical Survey Institute, 1987). Numerals show maximum shear strain and dilatation in 10^{-6}. Large open and closed circles denote the network and epicenter in 1961, respectively. The area enclosed by solid lines is the same as in Fig. 24.

roughly from NE-SW to E-W, and the magnitudes of the strains were about 10×10^{-6} over a period of about 100 years.

In the results of the secondary geodetic station surveys during the past 85 years shown in Fig. 24 (Geographical Survey Institute, 1977), however, the non-uniformity of strain distribution was conspicuous and the strains were greater than those shown in Fig. 23. Contractive strains in NE-SW direction are predominant in the zone along the Yasutomi fault, and extensional strains in the NW-SE direction are notable in the zone along the Kuresakatoge fault. These strain patterns are consistent with the left-lateral movements of the faults. The fact that the strains in small nets (as shown in Fig. 24) near the faults were greater than those in large nets (as shown in Fig. 23) which covers the same areas, suggests that strains concentrated in the neighborhood of the faults, and that their dislocations occurred in relatively narrow and shallow parts of the faults.

The largest earthquake which took place in the area along the Yamasaki fault system during the course of the measurements occurred in 1961. The magnitude of the earthquake was 5.9 and its epicenter was located about 25 km from the network as shown by a large closed circle in Fig. 23. This suggests that no major dislocation should occur on the Yasutomi fault or the Kuresakatoge fault.

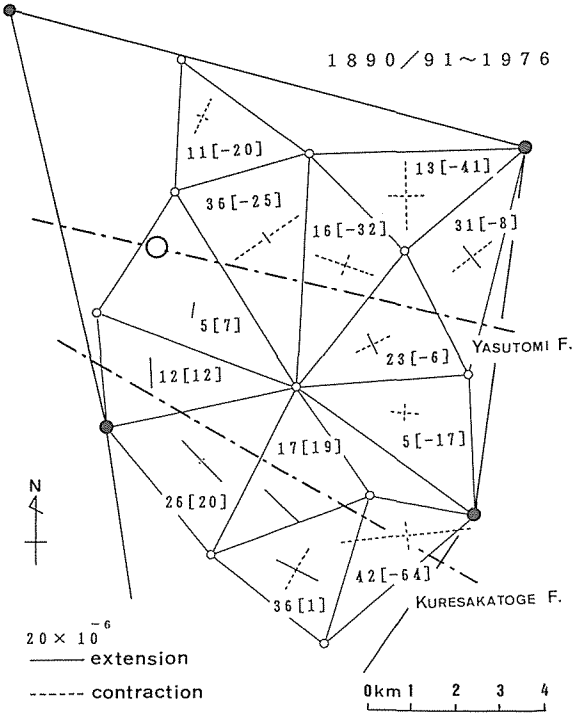

Fig. 24. Horizontal strain distribution obtained using the secondary geodetic stations around the Yasutomi and the Kuresakatoge faults (after Geographical Survey Institute, 1982). Numerals are the same as in Fig. 23. The large open circle denotes the network.

Accordingly, it is considered that the strains shown in Fig. 24 reflect the steady state of the faults, although they are very different from each other. This difference may be caused by the Quaternary movements of the two faults; that is, the Yasutomi fault dislocated left-laterally and vertically, while the Kuresakatoge fault dislocated only left-laterally.

A mean strain rate (on the order of 10^{-6} per year) obtained in the present network is about 10 times greater than the rate (on the order of 10^{-7} per year) estimated from those large-scale surveys near the Yasutomi fault. However, if the movements occur mainly in the vicinity of the fault, it is reasonable to expect that a large strain is obtained in the small network within the fracture zone of the fault.

From the considerations described previously and in this section, the movements of the Yasutomi fault are concluded as follows:

Some regions of the narrow and shallow part of the fault dislocate left-laterally and vertically. This movement manifests itself in the wide fracture zone of the fault. In the fracture zone, blocks move each other and amount of strain varies depending on the measurement location, larger in the fracture zone and smaller in outside of the zone.

8.3 Continuous Crustal Movements in the Yasutomi Tunnel

In the Yasutomi station (observation tunnel), continuous observations by an array of extensometers installed across the fracture zones of the Yasutomi fault have been carried out since 1975. Such observations have been monitoring the behavior of the fracture zones which are narrower than those discussed previously. Based on the measurement results, strain changes in the location were extensional in the NE-SW direction and contractive in the NW-SE direction. This suggests a right-lateral dislocation of the fracture zones. However, Watanabe (1991) concluded that no significant left-lateral creep movements of the Yasutomi fault occurred during the observation period.

Figure 25 shows strain changes observed employing the extensometers by Watanabe (1991). The strain changes in the same directions are extensional and contractive depending on the observed sites, similar to the non-uniformity in strains obtained by the geodetic measurements of the network. Further, Watanabe (1991) considered that, since the strain rate of some highly fractured portions in the basement rocks reached about 1×10^{-5} per year, the behavior of those portions was non-elastic. According to Oike (1977), a right-lateral slip motion of the fracture zone was observed by the extensometers after an isolated rainfall in a dry season during the few days before an increase in the activity of microearthquakes along the Yamasaki fault system.

These facts seem to suggest that each fracture zone of the Yasutomi fault shows

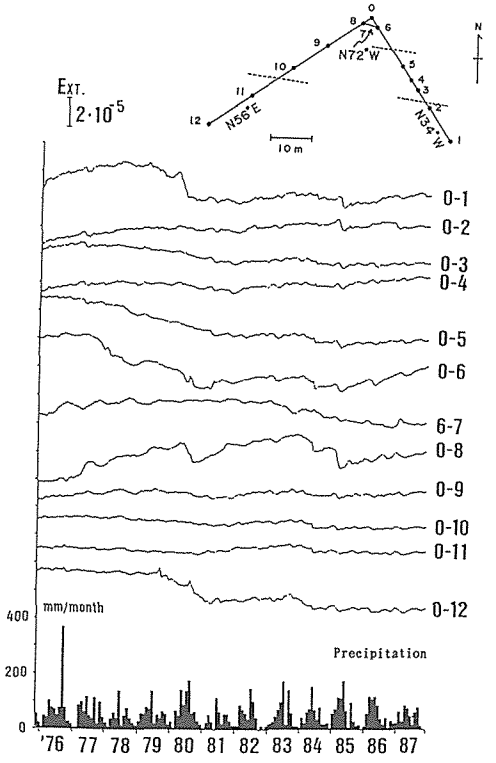

Fig. 25. Secular strain changes observed by extensometers in Yasutomi station (observation tunnel). The extensometers are crossing the fracture zone of the Yasutomi fault (after Watanabe, 1991).

the characteristic behavior of strain changes corresponding to each circumstance of the fracture zones; that is, stress fields, ground water levels, the modulus of elasticity, the coefficient of plastic flow and so on.

8.4 Stress Field around the Network

The focal mechanisms of earthquakes show that the maximum compressive stress affecting the Yamasaki fault system is in a direction nearly E-W (Ichikawa, 1971; Kishimoto and Nishida, 1973). *In situ* stress has not been measured around the fault system, but some measurements of the direction of the maximum compressive stress were made in the northwestern part of the Kinki District (Tanaka, 1986), showing roughly ESE-WNW. Therefore, it is anticipated that the direction of the major contractive strain axis in the network area is between E-W and ESE-WNW.

The direction of the major contractive axis (S50° E-N 50° W) in the network as a whole for about 14 years is roughly consistent with that expected from the stress fields, although the distribution of the strains in the network differs greatly.

9. Discussion

The hypothesis that plastic flows occur in the fracture zone of the fault was introduced in order to interpret the measurement results. There are no data at present which suggest that plastic flows occur in such a manner.

However, the phenomenon described, in which contraction and extension occur in the same direction at areas adjacent to each other, cannot be understood within the theory of elasticity. This phenomenon occurs within a violent fracture zone where the uniformity of materials cannot be expected. Further, permeability to water is high in the fracture zone due to many pores of various sizes. Fault clay also exists and the fault clay forced out from the fault fracture zone is sometimes observed. It is appropriate to consider, based on these facts, that there are plastic flows. Since the speed of plastic flows is independent of stress, the strain can be either extensional or contractive, with differences in locations occurring even between sites located near each other.

The plastic flows are considered to relate to the large width of the fracture zone, because a certain width is required for movements over a long duration. Perhaps, the plastic flows may not be observed very often in faults with sharp traces. This characteristic of the fracture zone seems to be closely related to the strain and tilt changes associated with earthquakes.

There is no perfect theory to explain the stress or strain changes within the crust prior to an earthquake. However, many precursors have been reported and formulated. Rikitake (1979) expressed them in terms of the time from the appearance of a phenomenon to an earthquake and the magnitude of the earthquake. Zhang and Fu (1981) reported successful prediction of several great earthquakes based on the geodetic measurements in China. These indicate that stresses or strains change within the crust before an earthquake.

Regarding precursors recorded prior to the 1984 earthquake (M = 5.6) occurred near the network, there was a seismic gap during the period of about a half year before the earthquake (Tsukuda, 1985). An episodic change in electric potential differences was observed about 40 days before the earthquake (Miyakoshi, 1986). Contractive strain changes observed by the extensometes at the Yasutomi observation tunnel during the period of about 8 months before the earthquake (Watanabe, 1991). These facts are consistent with the present results.

It is considered that stress increase in the crust causes both the plastic flows in the violent fracture zone and the earthquakes near the network, because the plastic flows occur near the ground surface, but the earthquakes take place at depth of about 20 km. Further usual strain changes (plastic flows do not occur) in the fracture zone are considered to be small. Crustal movements within the fracture zone may be closely related to local seismic activity.

The following conclusions of the fault movements were finally made based on the measurement results.

Blocks on both sides of the Yasutomi fault do not move relatively on a single line, but blocks within the fracture zone move rather individually within the wide sheared zone. This phenomenon causes severe strains and tilts in violent fracture zones within the sheared zone. Further, during the period from about 1 year before a nearby earthquake to about 2 years after the earthquake, the strain and tilt rates are large.

A long fault is usually consists of many echelon faults. This may apply by an analogy to the narrow portion of the fault as well. Also, violent fracture zones exist within the sheared zone of the fault. These zones are thought to be short in length and to cause the movements which occurred in the shallow section.

The analysis of seismic waveforms shows the existence of asperities on fault planes (e.g., Kanamori, 1981; Aki, 1984). Further, from the analysis of micro-earthquakes, the existence of asperities was inferred by Nishigami (1987). Perhaps, asperities of the fault exist also in the shallow section where no microearthquakes occur, and some fracture zones of the fault are susceptible to the movements and others are not.

It is considered that the present topography has been formed by such movements of the fault in the Quaternary period. In other words, movements which form this topography are necessary in order to preserve a minute topography, otherwise the minute topography would be ambiguous due to erosion.

We will have to wait for some time until the study reveals whether or not movements observed in the Yasutomi fault can be applicable to other inland faults.

10. Concluding Remarks

In order to study the crustal movements across the Yasutomi fault in the Yamasaki fault system in southwestern Japan, precise geodetic measurements have been carried out once a year since 1975 on a small baseline network across the fault. The results obtained during the period of about 14 years from 1975 to 1989

are summarized as follows:

(1) The strain rate of the network is on the order of 10^{-6} per year as a whole. This rate is one order of magnitude larger than the rate obtained by geodetic surveys with baselines of over several kilometers in the area concerned, and also one order of magnitude smaller than the rate observed by extensometers of several meters long across violent fracture zones of the fault.

(2) The distribution of strains within the network varies spatially and temporally, particularly in the NE-SW direction, with the northeastern part of the network showing contraction and the southwestern part showing extension. Such a non-uniformity of the strain distribution was also observed by the geodetic survey and the extensometers.

(3) The northeastern part of the network showed a tendency to upheave relative to the southwestern part. This is consistent with the Quaternary movements of the fault.

(4) The southern part of the network was also found to have rotated in a counterclockwise direction relative to the northern part, moving 2 or 3 seconds during the past 14 years.

(5) The episodic strain and height changes observed in the present study were related to seismic activity near the network. Speaking in detail, dilatation rates were compressive about one year before two moderate earthquakes ($M = 3.7$ and $M = 5.6$) with epicentral distances about 3 km from the network. Also, upheavals toward the epicenters were detected. At the time of the earthquakes, dilatation rates were expansive and the upheavals were recovered.

The movements and properties of the fault were concluded as follows:

Non-uniform spatial and temporal strain distribution as well as strain accumulation and release exist in and around the fault zone. These are caused by the small magnitude of the modulus of elasticity of the fault fracture zone compared to that in the surrounding crust, and plastic flows occurring within the violent fracture zone. Perhaps, the plastic flows start when the stress in the fracture zone exceeds a critical stress prior to the occurrence of an earthquake.

The Yasutomi fault has a wide fracture zone which is thought to be a sheared zone. The minute topography within the fracture zone is a good indication for the type of fault movements since the movements continue to shape the topography. These movements are probably linked to small and moderate earthquakes that occur nearby and are interpreted as a series of seismic cycles proposed by Lensen (1971). Judging from the small area in which these movements take place, they originate only in the shallow sections of the fault. Evidently, some fracture zones are susceptible to the movements and others are not.

As for a future guide for studying fault movements, a fault with a wide fracture zone such as the Yamasaki fault system requires the establishment of a network which has many stations and a large extent than the network established for the present study, to adequately study fault movements. The employment of GPS to measurements is strongly required. As for sites suitable for measurements, it is considered that fault intersections can sharply reflect stress changes and fault

behavior because vertical movements also occur there.

Acknowledgments

The present study was carried out under the support of the members of "the Research Group for the Yamasaki Fault" and those of the Laboratory of Physics of the Solid Earth, Department of Geophysics, Kyoto University. The author is grateful to the authorities of Yasutomi Town, Hyogo Prefecture and the Japan Expressway Corporation.

The author would like to thank Dr. Y. Tanaka and Professor I. Nakagawa for helpful advice and critical reading the manuscript. The author is also grateful to Mr. K. Iwasaki for his help and guidance in the measurements. The author wishes to acknowledge valuable discussions with Professors N. Sumitomo, T. Tanaka, K. Oike, S. Takemoto, S. Otsuka and M. Omura as well as Mr. K. Nakamura.

Numerical calculations were performed with the computer system at the Data Processing Center of Kyoto University.

References

Aki, K.: Asperities, Barriers, Characteristic Earthquakes and Strong Motion Prediction. J. Geophys. Res., **89**, 5867–5872, 1984.

Ando, M.: A Fault-Origin Model of the Great Kanto Earthquake of 1923 as Deduced from Geodetic Data. Bull. Earthq. Res. Inst., Univ. Tokyo, **49**, 19–32, 1971.

Dragomir, V. C., D. N. Ghitau, M. S. Mihailescu and M. G. Rotaru: Theory of the Earth's Shape. Developments in Solid Earth Geophysics 13, Elsevier, Amsterdam, 300, 1982.

Electromagnetic Research Group for the Active Fault: Low Electrical Resistivity along an Active Fault, the Yamasaki Fault. J. Geomag. Geoelectr., **34**, 103–127, 1982.

Fitch, T. J. and C. H. Scholz: Mechanism of Underthrusting in Southwest Japan: A Model of Convergent Plate Interactions. J. Geophys. Res., **76**, 7260–7292, 1971.

Fujimori, K., K. Nakamura, Y. Tanaka, S. Otsuka, E. Saito and K. Iwasaki: A Precise Geodetic Survey at the Yasutomi-Usuzuku Base Line Net across the Yamasaki Fault. J. Geod. Soc. Japan, **27**, 317–319, 1981.

Fukui, K.: Fault Topography along the Yamasaki Fault System, Western Kinki District, Japan. Geograph. Rev. Japan, **54**, 196–213, 1981. (in Japanese)

Geographical Survey Institute: Horizontal Strains around Yamazaki Fault. Rept. Coord. Comm. Earthq. Predict., **18**, 111–112, 1977. (in Japanese)

Geographical Survey Institute: Horizontal Strain in Japan, 1985–1883. Geogr. Surv. Inst., 75, 1987. (in Japanese)

Handa, S. and N. Sumitomo: The Geoelectric Structure of the Yamasaki and the Hanaori Faults, Southwest Japan. J. Geomag. Geoelectr., **37**, 93–106, 1985.

Hayashi, T.: A Study on the Vertical Movements of the Earth's Crust by Means of the Precise Leveling. Bull. Geogr. Surv. Inst., **15**, 1–67, 1969.

Huzita, K.: Tectonic Development of Southwest Japan in the Quaternary Period. J. Geosciences, Osaka City Univ., **12**, 53–70, 1969.

Huzita, K.: Yamasaki Fault System. Proc. Earthquake Prediction Research Symposium (1980), 143–147, 1980. (in Japanese)

Ichikawa, M.: Reanalyses of Mechanism of Earthquakes which Occurred in and near Japan, and Statistical Studies on the Nodal Plane Solutions Obtained, 1926–1968. Geophys. Mag., **35**, 207–274, 1971.

Ishii, H., A. Takagi and Z. Suzuki: Characteristic Movement of Crustal Deformation in Northeast Honshu, Japan. Gerlands Beitr. Geophys., **88**, 163–169, 1979.

Ishikawa, Y., K. Matsumura and H. Matsumoto: SEIS-PC —Its Outline—. Jyoho Chishitsu, **10**, 19–34, 1985. (in Japanese)

Jaeger, J. C.: Elasticity, Fracture and Flow, with Engineering and Geological Applications. Methuen & Co. Ltd., London, 98, 1964.

Kanamori, H.: The Nature of Seismicity Patterns before Major Earthquakes. Earthquake Prediction, An International Review, Maurice Ewing Series 1, Amer. Geophys. Union, Washington, D.C., 1–19, 1981.

Kasahara, K.: Migration of Crustal Deformation. Tectonophysics, **52**, 329–341, 1979.

King, N. E., P. Segall and W. Prescott: Geodetic Measurements near Parkfield, California, 1959–1984. J. Geophys. Res., **92**, 2747–2766, 1987.

Kinugasa, Y.: Crustal Strain on and around an Active Fault —An Example from the Survey on the Kitatake Fault—. J. Geod. Soc. Japan, **27**, 309–311, 1981.

Kishimoto, Y.: On Precursory Phenomena Observed at the Yamasaki Fault, Southwest Japan, as a Test-Field for Earthquake Prediction. Earthquake Prediction, An International Review, Maurice Ewing Series 4, Amer. Geophys. Union, Washington, D.C., 510–516, 1981.

Kishimoto, Y.: The Earthquake of M5.6 at the Yamasaki Fault, May 30, 1984. Proc. Earthquake Prediction Research Symposium (1987), 101–107, 1987. (in Japanese)

Kishimoto, Y. and R. Nishida: Mechanisms of Microearthquakes and Their Relation to Geological Structure. Bull. Disas. Prev. Res. Inst., Kyoto Univ., **23**, 1–25, 1973.

Lensen, G. J.: Phase, Nature and Rates of Earth Deformation, Recent Crustal Movements. Roy. Soc. New Zeal., Bull., **9**, 97–105, 1971.

Miyakoshi, J.: Anomalous Time Variation of the Self-Potential in the Fractured Zone of an Active Fault Preceding the Earthquake Occurrence. J. Geomag. Geoelectr., **38**, 1015–1030, 1986.

Nakane, K.: Horizontal Tectonic Strain in Japan (I). J. Geod. Soc. Japan, **19**, 190–199, 1973a. (in Japanese)

Nakane, K.: Horizontal Tectonic Strain in Japan (II). J. Geod. Soc. Japan, **19**, 200–208, 1973b. (in Japanese)

Nishida, R.: The Focal Mechanisms of the Earthquakes. The Earth Monthly, **7**, 49–53, 1985. (in Japanese)

Nishigami, K.: Clustering Structure and Fracture Process of Microearthquake Sequences. J. Phys. Earth, **35**, 425–448, 1987.

Nishimura, S., T. Mogi, K. Mino and T. Sadahiro: Diagnosis of Active Fault —The Yamasaki Fault System—. Ann. Disas. Prev. Res. Inst., Kyoto Univ., **28B-1**, 91–97, 1985. (in Japanese)

Oike, K.: Seismic Activities and Crustal Movements at the Yamasaki Fault and Surrounding Regions in the Southwest Japan. J. Phys. Earth, **25**, S31–S41, 1977.

Okada, A., M. Ando and T. Tsukuda: Trenches across the Yamasaki Fault in Hyogo Prefecture. Rept. Coord. Comm. Earthq. Predict., **24**, 190–194, 1980. (in Japanese)

Omura, M., K. Fujimori, S. Otsuka, K. Nakamura and Y. Tanaka: Geodetic Monitoring of the Crustal Movements across the Yamasaki Fault, Southwest Japan. Bull. Disas. Prev. Res. Inst., Kyoto Univ., **38**, 79–97, 1988.

Omura, M., K. Fujimori, Y. Tanaka and S. Otsuka: Electro-Optical Distance Measurements by Using a Geomensor CR204 —Yasutomi-Usuzuku Baseline Network, Yamasaki Fault, Southwest Japan—. J. Geod. Soc. Japan, **35**, 307–317, 1989. (in Japanese)

Otsuka, S., Y. Tamura, K. Fujimori and Y. Tanaka: Crustal Deformations Observed at the Rokko-Tsurukabuto Observation Station (I). J. Geod. Soc. Japan, **28**, 134–151, 1982. (in Japanese)

Rikitake, T.: Classification of Earthquake Precursors. Tectonophysics, **54**, 293–309, 1979.

Savage, J. C. and R. O. Burford: Geodetic Determination of Relative Plate Motion in central California, J. Geophys. Res., **78**, 832–845, 1973.

Tanaka, Y.: State of Crustal Stress Inferred from *In Situ* Stress Measurements, J. Phys. Earth, **34**, S57–S70, 1986.

Tanaka, Y.: Modes of Crustal Movements in Subduction Zones —Observed Results in the Kii Peninsula along the Nankai Trough—. J. Geod. Soc. Japan, **35**, 133–147, 1989.

Tanaka, Y., M. Hayashi, M. Kato, M. Koizumi and K. Huzita: Continuous Observation of Crustal Deformations in a Fracture Zone of Rokko Fault System (Preliminary Report). Ann. Disas. Prev. Res. Inst., Kyoto Univ., **15B**, 15–28, 1972. (in Japanese)

Thatcher, W.: Systematic Inversion of Geodetic Data in Central California. J. Geophys. Res., **84**, 2283–2295, 1979.

The Research Group for Active Faults: Active Faults in Japan, the University of Tokyo Press, Tokyo, 363 p., 1980. (in Japanese)

Tsukuda, T.: V_p/V_s Anomaly around the Source Region of the Earthquake of M3.7 on September 30, 1977, in the Vicinity of the Yamasaki Fault. Ann. Disas. Prev. Res. Inst., Kyoto Univ., **21B–1**, 27–36, 1978. (in Japanese)

Tsukuda, T.: Seismic Activity along the Yamasaki Fault. The Earth Monthly, **7**, 9–14, 1985. (in Japanese)

Watanabe, K.: Strain Variations of the Yamasaki Fault Zone, Southwest Japan, Derived from the Extensometer Observations, Part 1 —On the Long-Term Strain Variations—. Bull. Disas. Prev. Res. Inst., Kyoto Univ., **41**, 29–52, 1991.

Zhang, G. and Z. Fu: Some Features of Medium- and Short-Term Anomalies before Great Earthquakes. Earthquake Prediction, An International Review, Maurice Ewing Series 4, Amer. Geophys. Union, Washington, D.C., 497–509, 1981.

Table 1. Adjusted coordinates from 1975 to 1989

The coordinates were determined by free network adjustments, based on the coordinates determined in December 1975. Station 1 was fixed in the estimation of height. The "SD" indicates one standard deviation. Triangles W1 to W5 are the same as in Fig. 4.

December 7～16, 1975

	Adjusted Coordinates						Misclosure
Station	x	[SD]	y	[SD]	z	[SD]	△W1 -0.37"
	m	mm	m	mm	m	mm	W2 -1.68
1	0.00000	[0.48]	0.00000	[0.37]	187.98430	[0.29]	W3 -0.32
2	68.03712	[0.50]	-30.86715	[0.33]	183.24478	[0.25]	W4 -0.05
3	189.01715	[0.64]	-191.63790	[0.64]	202.88889	[0.39]	W5 -1.59
4	70.01452	[0.64]	-166.33451	[0.54]	185.40079	[0.33]	SD of
5	166.75244	[0.29]	129.33489	[0.76]	198.63671	[0.41]	baseline 1-2
6	321.60525	[0.77]	56.12160	[0.59]	214.95306	[0.48]	0.024mm

November 29 ～ December 8, 1976

	Adjusted Coordinates						Misclosure
Station	x	[SD]	y	[SD]	z	[SD]	△W1 -0.21"
	m	mm	m	mm	m	mm	W2 0.78
1	0.00096	[0.37]	-0.00009	[0.27]	187.98430	[0.28]	W3 -1.40
2	68.03797	[0.38]	-30.86679	[0.25]	183.24491	[0.24]	W4 -0.25
3	189.01778	[0.44]	-191.63609	[0.55]	202.88824	[0.38]	W5 -1.39
4	70.01414	[0.45]	-166.33411	[0.45]	185.40040	[0.32]	SD of
5	166.75250	[0.24]	129.33351	[0.66]	198.63771	[0.40]	baseline 1-2
6	321.60330	[0.67]	56.12067	[0.49]	214.95252	[0.47]	0.050mm

December 6～14, 1977

	Adjusted Coordinates						Misclosure
Station	x	[SD]	y	[SD]	z	[SD]	△W1 -0.77"
	m	mm	m	mm	m	mm	W2 -0.43
1	0.00040	[0.41]	-0.00067	[0.22]	187.98430	[0.33]	W3 0.67
2	68.03773	[0.41]	-30.86652	[0.20]	183.24562	[0.28]	W4 0.40
3	189.01793	[0.32]	-191.63621	[0.78]	202.88834	[0.43]	W5 -0.89
4	70.01406	[0.41]	-166.33410	[0.60]	185.40108	[0.37]	SD of
5	166.75283	[0.20]	129.33401	[0.79]	198.63749	[0.45]	baseline 1-2
6	321.60370	[0.93]	56.12060	[0.49]	214.95386	[0.53]	0.024mm

November 14～21, 1978

	Adjusted Coordinates						Misclosure
Station	x	[SD]	y	[SD]	z	[SD]	△W1 -0.47"
	m	mm	m	mm	m	mm	W2 0.43
1	0.00035	[0.40]	-0.00015	[0.32]	187.98430	[0.47]	W3 0.05
2	68.03774	[0.42]	-30.86538	[0.30]	183.24590	[0.40]	W4 0.16
3	189.01806	[0.57]	-191.63663	[0.47]	202.88956	[0.62]	W5 -0.50
4	70.01457	[0.54]	-166.33490	[0.41]	185.40097	[0.53]	SD of
5	166.75249	[0.26]	129.33424	[0.52]	198.63897	[0.65]	baseline 1-2
6	321.60374	[0.55]	56.12073	[0.48]	214.95532	[0.77]	0.000mm

November 13～20, 1979

	Adjusted Coordinates						Misclosure
Station	x	[SD]	y	[SD]	z	[SD]	△W1 0.32"
	m	mm	m	mm	m	mm	W2 0.26
1	0.00062	[0.29]	-0.00029	[0.23]	187.98430	[0.33]	W3 -0.40
2	68.03781	[0.30]	-30.86565	[0.21]	183.24606	[0.28]	W4 -0.12
3	189.01862	[0.41]	-191.63594	[0.34]	202.88927	[0.44]	W5 -1.07
4	70.01356	[0.39]	-166.33457	[0.29]	185.40105	[0.38]	SD of
5	166.75277	[0.19]	129.33389	[0.38]	198.63906	[0.47]	baseline 1-2
6	321.60317	[0.40]	56.12058	[0.35]	214.95603	[0.55]	0.036mm

November 18～27, 1980

	Adjusted Coordinates						Misclosure
Station	x	[SD]	y	[SD]	z	[SD]	△W1 1.26"
	m	mm	m	mm	m	mm	W2 -0.17
1	0.00088	[0.40]	-0.00026	[0.33]	187.98430	[0.32]	W3 -0.46
2	68.03811	[0.43]	-30.86560	[0.30]	183.24604	[0.27]	W4 0.08
3	189.01859	[0.58]	-191.63545	[0.48]	202.88899	[0.42]	W5 -1.96
4	70.01394	[0.55]	-166.33474	[0.41]	185.40139	[0.36]	SD of
5	166.75261	[0.26]	129.33376	[0.53]	198.63894	[0.44]	baseline 1-2
6	321.60314	[0.56]	56.12047	[0.49]	214.95560	[0.52]	0.059mm

November 16～25, 1981

	Adjusted Coordinates						Misclosure
Station	x	[SD]	y	[SD]	z	[SD]	△W1 -0.13"
	m	mm	m	mm	m	mm	W2 0.26
1	0.00108	[0.35]	-0.00059	[0.29]	187.98430	[0.16]	W3 0.05
2	68.03841	[0.37]	-30.86557	[0.26]	183.24544	[0.14]	W4 -0.77
3	189.01828	[0.51]	-191.63549	[0.42]	202.88899	[0.21]	W5 -1.08
4	70.01399	[0.48]	-166.33422	[0.36]	185.40183	[0.18]	SD of
5	166.75233	[0.23]	129.33380	[0.47]	198.63941	[0.22]	baseline 1-2
6	321.60279	[0.49]	56.12007	[0.43]	214.95622	[0.26]	0.065mm

November 17～26, 1982

	Adjusted Coordinates						Misclosure
Station	x	[SD]	y	[SD]	z	[SD]	△W1 0.73"
	m	mm	m	mm	m	mm	W2 -0.21
1	0.00064	[0.33]	-0.00044	[0.27]	187.98430	[0.23]	W3 0.26
2	68.03825	[0.35]	-30.86555	[0.24]	183.24570	[0.20]	W4 0.76
3	189.01805	[0.47]	-191.63545	[0.39]	202.88953	[0.30]	W5 -1.32
4	70.01397	[0.45]	-166.33471	[0.34]	185.40180	[0.26]	SD of
5	166.75253	[0.21]	129.33407	[0.43]	198.63851	[0.32]	baseline 1-2
6	321.60323	[0.45]	56.12045	[0.40]	214.95534	[0.37]	0.046mm

November 16～24, 1983

	Adjusted Coordinates						Misclosure
Station	x	[SD]	y	[SD]	z	[SD]	△W1 -0.16"
	m	mm	m	mm	m	mm	W2 0.17
1	0.00129	[0.25]	-0.00072	[0.21]	187.98430	[0.25]	W3 -0.67
2	68.03879	[0.27]	-30.86574	[0.19]	183.24543	[0.21]	W4 -0.01
3	189.01842	[0.37]	-191.63462	[0.31]	202.88912	[0.33]	W5 -0.67
4	70.01422	[0.35]	-166.33397	[0.26]	185.40219	[0.28]	SD of
5	166.75284	[0.17]	129.33318	[0.34]	198.63831	[0.35]	baseline 1-2
6	321.60187	[0.35]	56.11989	[0.31]	214.95423	[0.41]	0.024mm

November 16～24, 1984

Station	Adjusted Coordinates x [SD]	y [SD]	z [SD]	Misclosure
	m mm	m mm	m mm	△W1 0.54"
1	0.00067 [0.56]	-0.00145 [0.46]	187.98430 [0.30]	W2 -1.10
2	68.03925 [0.60]	-30.86506 [0.42]	183.24469 [0.26]	W3 -0.32
3	189.01838 [0.82]	-191.63538 [0.68]	202.88980 [0.40]	W4 -0.62
4	70.01337 [0.78]	-166.33418 [0.58]	185.40128 [0.35]	W5 -1.82
5	166.75266 [0.37]	129.33391 [0.75]	198.63961 [0.42]	SD of
6	321.60296 [0.78]	56.12054 [0.68]	214.95669 [0.50]	baseline 1-2
				0.094mm

November 20～29, 1985

Station	Adjusted Coordinates x [SD]	y [SD]	z [SD]	Misclosure
	m mm	m mm	m mm	△W1 0.39"
1	0.00111 [0.44]	-0.00169 [0.36]	187.98430 [0.20]	W2 0.38
2	68.03964 [0.47]	-30.86515 [0.33]	183.24427 [0.17]	W3 -0.73
3	189.01858 [0.64]	-191.63460 [0.53]	202.88874 [0.26]	W4 0.20
4	70.01325 [0.61]	-166.33353 [0.45]	185.40073 [0.22]	W5 -1.77
5	166.75283 [0.29]	129.33311 [0.58]	198.63836 [0.27]	SD of
6	321.60196 [0.61]	56.12014 [0.53]	214.95501 [0.32]	baseline 1-2
				0.028mm

November 20～27, 1986

Station	Adjusted Coordinates x [SD]	y [SD]	z [SD]	Misclosure
	m mm	m mm	m mm	△W1 0.70"
1	0.00176 [0.35]	-0.00216 [0.29]	187.98430 [0.33]	W2 0.01
2	68.04025 [0.37]	-30.86520 [0.26]	183.24428 [0.28]	W3 0.00
3	189.01788 [0.51]	-191.63361 [0.42]	202.89030 [0.44]	W4 -0.51
4	70.01370 [0.48]	-166.33275 [0.36]	185.40154 [0.38]	W5 -1.29
5	166.75270 [0.23]	129.33256 [0.47]	198.63954 [0.46]	SD of
6	321.60101 [0.49]	56.11971 [0.43]	214.95711 [0.54]	baseline 1-2
				0.031mm

November 18～26, 1987

Station	Adjusted Coordinates x [SD]	y [SD]	z [SD]	Misclosure
	m mm	m mm	m mm	△W1 0.20"
1	0.00197 [0.45]	-0.00212 [0.37]	187.98430 [0.32]	W2 -0.98
2	68.04042 [0.48]	-30.86515 [0.34]	183.24440 [0.27]	W3 -0.31
3	189.01763 [0.65]	-191.63349 [0.54]	202.88956 [0.42]	W4 -0.02
4	70.01418 [0.62]	-166.33315 [0.46]	185.40219 [0.36]	W5 -1.25
5	166.75278 [0.29]	129.33238 [0.60]	198.63923 [0.44]	SD of
6	321.60093 [0.63]	56.11978 [0.55]	214.95608 [0.52]	baseline 1-2
				0.035mm

November 17～23, 1988

Station	Adjusted Coordinates x [SD]	y [SD]	z [SD]	Misclosure
	m mm	m mm	m mm	△W1
1	0.00167 [0.13]	-0.00215 [0.16]	187.98430 [0.49]	W2
2	68.04007 [0.13]	-30.86506 [0.14]	183.24431 [0.46]	W3
3	189.01797 [0.16]	-191.63281 [0.18]	202.88998 [0.55]	W4
4	70.01358 [0.15]	-166.33287 [0.14]	185.40150 [0.51]	W5
5	166.75270 [0.14]	129.33254 [0.20]	198.64006 [0.56]	SD of
6	321.60100 [0.12]	56.11951 [0.18]	214.95635 [0.60]	baseline 1-2
				0.043mm

November 23～27, 1989

Station	Adjusted Coordinates x [SD]	y [SD]	z [SD]	Misclosure
	m mm	m mm	m mm	△W1
1	0.00169 [0.09]	-0.00231 [0.12]	187.98430 [0.41]	W2
2	68.04008 [0.10]	-30.86517 [0.11]	183.24436 [0.38]	W3
3	189.01775 [0.13]	-191.63278 [0.14]	202.88931 [0.45]	W4
4	70.01404 [0.12]	-166.33285 [0.11]	185.40135 [0.42]	W5
5	166.75285 [0.09]	129.33262 [0.13]	198.63840 [0.46]	SD of
6	321.60078 [0.09]	56.11916 [0.14]	214.95551 [0.50]	baseline 1-2
				0.070mm